Understanding eigenfrequency shifts observed in vortex gyrotropic motions in a magnetic nanodot driven by spin-polarized out-of-plane dc current

Youn-Seok Choi, Sang-Koog Kim, Ki-Suk Lee, and Young-Sang Yu

Citation: Applied Physics Letters **93**, 182508 (2008); doi: 10.1063/1.3012380

View online: http://dx.doi.org/10.1063/1.3012380

View Table of Contents: http://scitation.aip.org/content/aip/journal/apl/93/18?ver=pdfcov

Published by the AIP Publishing

Understanding eigenfrequency shifts observed in vortex gyrotropic motions in a magnetic nanodot driven by spin-polarized out-of-plane dc current

Youn-Seok Choi, Sang-Koog Kim,[a] Ki-Suk Lee, and Young-Sang Yu
Research Center for Spin Dynamics and Spin-Wave Devices and Nanospinics Laboratory, Department of Materials Science and Engineering, College of Engineering, Seoul National University, 151-744 Seoul, Republic of Korea

(Received 22 August 2008; accepted 11 October 2008; published online 7 November 2008)

We observed sizable eigenfrequency shifts in spin-polarized dc-current-driven vortex gyrotropic motions in a soft magnetic nanodot, and clarified the underlying physics through micromagnetic numerical calculations. It was found that the vortex eigenfrequency is changed to higher (lower) values with increasing Oersted field (OH) strength associated with the out-of-plane dc current for the vortex chirality parallel (antiparallel) to the rotation sense of the OH circumferential in-plane orientation. The eigenfrequency shift was found to be linearly proportional to the current density j_0 in the linear regime as in $\Delta\nu_D \simeq \pm \eta j_0/|G|$, where G is the gyrovector constant and η is a positive constant, e.g., 1.9×10^{-8} erg/A for a model Permalloy dot of 300 nm diameter and 20 nm thickness. This behavior originates from the sizable contribution of the OH to the effective potential energy of a displaced vortex core in the gyrotropic motion. The present results reveal that ν_D, an intrinsic dynamic characteristic of a given nanodot vortex state, is controllable by changes in both the density and direction of spin-polarized out-of-plane dc currents. © *2008 American Institute of Physics*. [DOI: 10.1063/1.3012380]

Recent studies[1–6] have established that the spin-transfer torque (STT) of spin-polarized electric currents is a promisingly reliable means of switching the orientation of magnetizations (**M**) in magnetic particles of submicron size or less. The STT thereby has been practically used in information storage[1,7] devices, due to several advantages including low-power, ultrafast, and reliable information recording, and in frequency-tunable microwave oscillators.[4,7,8] Moreover, the STT effect on magnetic vortex excitations in nanodot and nanopillar systems has begun to receive a great deal of attention owing to its potential applications to future information storage and microwave oscillator devices.[9–20] For instance, the current-driven vortex gyrotropic oscillation[9–13] and vortex core (VC) **M** switching[14–20] in confined magnetic systems have been observed both experimentally[9–11,13,14] and numerically.[12,15–20] Despite the several studies conducted on the STT effect on such vortex excitations, quantitative understanding of the Oersted field (OH) effect of the spin-polarized currents has been lacking, even though this type of field has been reported to make sizable contributions to **M** reversals[5,21,22] and VC oscillations.[9,10,13]

In this letter, we report the observation of sizable shifts in the intrinsic eigenfrequency $\nu_D=(1/2\pi)\omega_\nu$, of vortex gyrotropic motions in a laterally confined thin-film nanodot. The physical origin of this behavior was quantitatively understood by considering the Zeeman contribution of the spin-polarized-current-induced circumferential OH to the effective potential energy of a displaced VC. We found an analytical equation that relates the eigenfrequency shift to the current density and its flowing direction. The present work provides a reliable means of manipulating ν_D, of a given vortex state by using spin-polarized out-of-plane dc currents, which manipulation that might be applicable to frequency-tunable oscillators in the subgigahertz range without additionally applied magnetic fields.

To conduct micromagnetic numerical calculations of vortex dynamics associated with a low-frequency translation mode (the so-called gyrotropic motion) in a nanodot, we used the LLG code,[23] which utilizes the Landau–Lifshitz–Gilbert equation of motion, which includes the STT term,[1,2] expressed as $\mathbf{T}_{\mathrm{STT}}=(a_{\mathrm{STT}}/M_s)\mathbf{M}\times(\mathbf{M}\times\hat{\mathbf{m}}_{\mathrm{P}})$, with $a_{\mathrm{STT}}=(1/2\pi)h\gamma P j_0/(\mu_0 2eM_sL)$. $\hat{\mathbf{m}}_{\mathrm{P}}$ is the unit vector of the spin polarization orientation, h is the Planck constant, γ is the gyromagnetic ratio, P is the degree of spin polarization, j_0 is the current density, μ_0 is the vacuum permeability, e is the electron charge, M_s is the constant magnitude of **M**, and L is the thickness of a free magnetic layer. We employed, as a model, a circular-shaped Permalloy (Py) ($Ni_{80}Fe_{20}$) nanodot of $2R=300$ nm and $L=20$ nm [see Fig. 1(a)]. An equilibrium vortex state in the given dot can be characterized by the vortex integers of the chirality c and the polarization p: $c=+1$ (-1) corresponds to the counterclockwise (CCW) [clockwise (CW)] rotation sense of the in-plane curling **M**, and $p=+1$ (-1) corresponds to the upward (downward) **M**

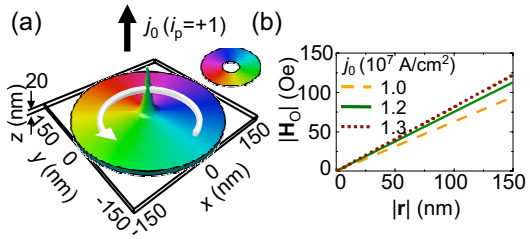

FIG. 1. (Color online) (a) Vortex state with upward **M** orientation of its VC and CCW in-plane curling **M** in circular Py dot of indicated dimensions. The color and height display the local in-plane **M** and out-of-plane **M** components, respectively. (b) OH strength profile along radial distance $|\mathbf{r}|$ for indicated different j_0 values.

[a]Author to whom correspondence should be addressed. Electronic mail: sangkoog@snu.ac.kr.

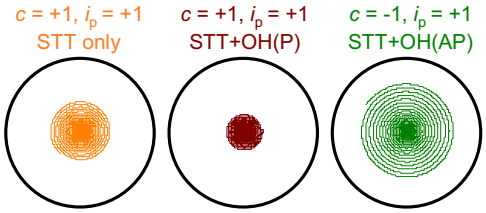

FIG. 2. (Color online) Orbital trajectories of moving VC under spin-polarized out-of-plane dc current of $j_0=1.3\times10^7$ A/cm^2 for indicated different cases, as noted in text and above each figure. Here, the chirality (c) of the vortex state and the rotation sense of the OH are noted above each figure.

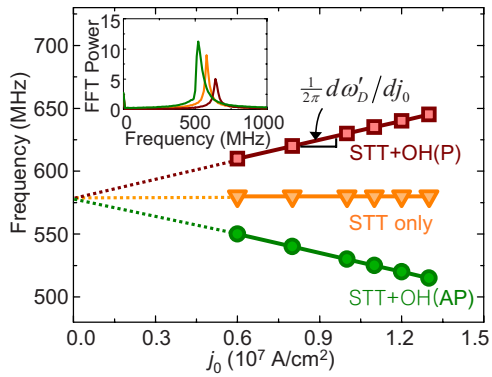

FIG. 3. (Color online) Dominant frequency variations with j_0 for three different cases. The inset shows the FFT power vs frequency, calculated from the time-varying x-component of the VC position under a spin-polarized current with $j_0=1.3\times10^7$ A/cm^2.

orientation of the VC. For example, the vortex state of $c=+1$ and $p=+1$ is illustrated in Fig. 1(a). In the present simulations, we used $p=+1$ and $\hat{\mathbf{m}}_P$ was in the $-z$ direction [antiparallel (AP) to the vortex polarization]. Spin-polarized currents were applied for 100 ns through the dot of the vortex state toward the $+z$ direction. Then, we investigated vortex gyrotropic motions in the linear regime.

In order to examine how the OH effect of out-of-plane dc currents is considerable in vortex gyrotropic motions, first we calculated the strength profile of the OH produced for different j_0 values based on Biot–Savart's formulation $\mathbf{H}_O(\mathbf{r})=(1/2)j_0 i_p(\hat{\mathbf{z}}\times\mathbf{r})$, where $\mathbf{r}$ is the radial vector from the center position ($\mathbf{r}=0$) and i_p is the direction of the applied currents, i.e., $i_p=+1$ (-1) corresponds to the $+z$ $(-z)$ direction. The CCW and CW rotation senses of the circumferential OH are thus determined simply by the sign of i_p, i.e., corresponding to $i_p=+1$ and -1, respectively. For $i_p=\pm1$, the OH strength profile versus $|\mathbf{r}|$ for different j_0 values are shown in Fig. 1(b). At the center of the dot, $|\mathbf{H}_O(0)|=0$ for all of the j_0 values, but sufficiently large values of $\sim$100 Oe are obtained at the edge, which values can modify vortex gyrotropic motions.

Figure 2 displays the orbital trajectories of the spiral motions of a VC in the linear regime driven by a spin-polarized current with $j_0=1.3\times10^7$ A/cm^2 for the three different indicated cases: only the STT effect in the absence of the OH and the STT effect considering the OH with its circumferential in-plane orientation parallel (P) and AP to a given vortex chirality ($c=+1$ or -1). These three different cases hereafter are abbreviated as case I, "STT only;" case II, "STT+OH(P);" and case III, "STT+OH(AP)." For all of the cases, the observed orbital trajectories show spirally rotating motions with *exponentially increasing* orbital radii. In cases of in-plane oscillating currents[11,14,16–18] or fields,[17,24,25] the increasing orbital radius converges exponentially to a certain steady-state orbital radius.[16,17,24] In contrast, the out-of-plane spin-polarized current-driven vortex gyrotropic motions show exponentially increasing orbital radii with distinctive rates for the different cases of I, II, and III. Such an exponentially increasing orbital radius[26] is one of the characteristic dynamic properties of spin-polarized out-of-plane current-driven vortex gyrotropic motions.

From fast Fourier transforms (FFTs) of the time variation of the x-component of the VC position, we obtained FFT spectra as a function of the frequency. As revealed in the inset of Fig. 3, the eigenfrequencies and their full widths at half maximum (FWHMs) in cases I, II, and III are very contrasting. The value of $\nu_D=580$ MHz(FWHM: 30 MHz) in case I was shifted to a higher value, 645 MHz (FWHM: 50 MHz) in case II, and to a lower value of 515 MHz (FWHM: 40 MHz) in case III. In order to quantitatively clarify the observed OH effect on the eigenfrequency shifts, we plotted the modified eigenfrequency $(1/2\pi)\omega_D'$ as a function of j_0, for those j_0 values larger than a critical current density j_{cri}. Here j_{cri} is defined as a threshold current density above which the vortex gyrotropic motions can be excited with a continuously increasing orbital radius.[27] It is clearly shown that $(1/2\pi)\omega_D'$ increases (decreases) linearly with increasing OH strength for the P (AP) orientation between c and the rotation sense of OH (Fig. 3). From the linear fits (lines) to the simulation results (symbols), we could find a relationship between $(1/2\pi)\omega_D'$ and j_0. Note that $(1/2\pi)d\omega_D'/dj_0$ is zero for STT only (case I), and that for cases II and III, the values of $(1/2\pi)\omega_D'$ converge to $(1/2\pi)\omega_D=580$ MHz, with the approach to $j_0=0$, according to the slope $(1/2\pi)d\omega_D'/dj_0=\pm5.0$ cm^2/A s. The sign of $(1/2\pi)d\omega_D'/dj_0$ is determined by the sign of the product of c and i_p, i.e., $ci_p=+1$ (-1) corresponding to the P (AP) orientation between the vortex chirality and the rotation sense of OH.

Next, in order to elucidate the underlying physics of the OH effect on the modification of the ω_D' value and to obtain a quantitative relation between ω_D' and j_0, we used the known relation $\omega_D\simeq\omega_0=\kappa_0/|G|$ for a small Gilbert damping parameter, e.g., here $\alpha=0.01$,[17,24] where G is the gyrovector constant and κ_0 is the intrinsic stiffness coefficient of the potential energy.[28] For a given dot, G and κ_0 are constant, 6.14×10^{-10} erg s/cm^2 and 2.3 erg/cm^2, respectively, for the model used in this study. Thus $(1/2\pi)\omega_0=596$ MHz, a value close to that (580 MHz) obtained from the simulation result. Therefore, the modified ω_D' values can be evaluated directly from the modified κ values due to the OH contribution. For a small displaced VC, the potential energy is given as $W(\mathbf{X})=W(0)+\kappa_0\mathbf{X}^2/2$, considering both the exchange and magnetostatic energies. To obtain the relation of the OH contribution to κ, the κ value can be determined from the plot of $W_{tot}(\mathbf{X})$ versus $|\mathbf{X}|^2$ (see the left top panel of Fig. 4), where the $W_{tot}(\mathbf{X})$ were obtained from the simulation results for cases I, II, and III. As seen in the right top panel of Fig. 4, it is evident that the Zeeman energy term modifies the slope of the W_{tot} versus $|\mathbf{X}|^2$ in each case. In contrast, the magnetostatic and exchange energy contributions to the modification of the $W_{tot}(\mathbf{X})$ versus $|\mathbf{X}|^2$ in cases I, II, and III are negligible.

The linear fits to the W_{tot} versus $|\mathbf{X}|^2$ for the different j_0 values allow us to numerically estimate the κ values according to j_0 for cases I, II, and III; these curves are plotted in

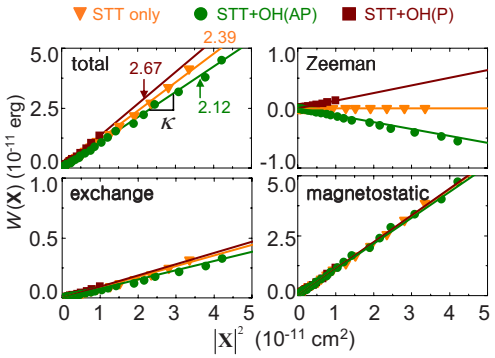

FIG. 4. (Color online) $W(\mathrm{X})$ vs $|\mathbf{X}|^2$ curves for total, individual Zeeman, exchange, and magnetostatic contributions for $j_0=1.3\times10^7$ A/cm^2. Each colored line indicates a linear fit to the corresponding simulation result (symbol) for each case. The linear fit values in the left top are as follows: $\boldsymbol{\kappa}$=2.39, 2.67, and 2.12 erg/cm^2 for cases I, II, and III, respectively.

Fig. 5. It is clear that $\boldsymbol{\kappa}$ for STT only is independent of j_0 (see inset) and thus it turns to be $\boldsymbol{\kappa}_0$ and numerically estimated to be 2.39 erg/cm^2. By contrast, in the two cases including the OH effect, the $\boldsymbol{\kappa}$ value varies linearly with j_0, thereby yielding the slope $d\boldsymbol{\kappa}/dj_0=\pm1.9\times10^{-8}$ erg/A. Consequently, the effective potential energy accounting for the OH effect can be rewritten as $W_{\mathrm{tot}}(\mathbf{X})=W_{\mathrm{tot}}(0)+[\kappa_0+\kappa_{\mathrm{OH}}]\mathbf{X}^2/2$, where $\boldsymbol{\kappa}_{\mathrm{OH}}$ is an additional term associated with the OH contribution. From the slopes of the $\boldsymbol{\kappa}$ versus j_0 curves shown in Fig. 5, we obtain $\boldsymbol{\kappa}_{\mathrm{OH}}=\pm\eta j_0$ with $\eta=1.9\times10^{-8}$ erg/A for the given Py dot, leading to the relation of $\omega_D'\simeq[\boldsymbol{\kappa}_0+\boldsymbol{\kappa}_{\mathrm{OH}}]/|G|=[\boldsymbol{\kappa}_0\pm\eta j_0]/|G|$. As a result, the eigenfrequency shift, $\Delta\omega_D=\omega_D'-\omega_D$, is given simply by $\Delta\omega_D\simeq\boldsymbol{\kappa}_{\mathrm{OH}}/|G|=\pm\eta j_0/|G|$. The value of $\Delta\omega_D$ is positive (negative) for the positive (negative) value of ci_{p}. The rotation sense of the OH relative to the vortex chirality affects $\boldsymbol{\kappa}$ for a vortex motion. It is given that for $ci_{\mathrm{p}}=+1$, $\boldsymbol{\kappa}_0+\boldsymbol{\kappa}_{\mathrm{OH}}>\boldsymbol{\kappa}_0$and for $ci_{\mathrm{p}}=-1$, $\boldsymbol{\kappa}_0+\boldsymbol{\kappa}_{\mathrm{OH}}<\boldsymbol{\kappa}_0$. From the estimated values of $\eta=|d\boldsymbol{\kappa}/dj_0|=1.9\times10^{-8}$ erg/A and $G=6.14\times10^{-10}$ erg s/cm^2 (Ref. 28) for the model dot used here, we obtained the value of $(1/2\pi)\eta/|G|=4.92$ cm^2/A s, which is in quite good agreement with the value of $(1/2\pi)|d\omega_D'/dj_0|=5.0$ cm^2/A s obtained from the observed eigenfrequency shifts shown in Fig. 3. Finally, we can relate the eigenfrequency shifts to the OH effect, as in the analytical form of $\Delta\omega_D\simeq(ci_{\mathrm{p}}\eta/|G|)j_0$. This result quantitatively verifies that the observed eigenfrequency shifts originate from the Zeeman contribution of the OH of spin-polarized currents to the potential energy stiffness coefficient, and vary with both the applied current density and its direction.

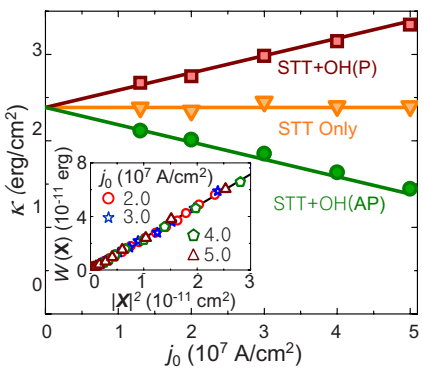

FIG. 5. (Color online) $\boldsymbol{\kappa}$ vs j_0 relationships for all three cases. The inset shows the total potential energy as a function of $|\mathbf{X}|^2$ for case I with different j_0 values.

To conclude, spin-polarized current density and its direction modify the intrinsic eigenfrequency of vortex gyrotropic motion in a given dot. From an application point of view, this eigenfrequency modification by the external driving force of spin-polarized dc currents without an additionally applied magnetic field can be applicable to frequency-tunable oscillators in the subgigahertz range.

Note added in proof: All numerical values of j_0 should be corrected by multiplying $\pi/4$.

This work was supported by Creative Research Initiatives (ReC-SDSW) of MEST/KOSEF.

[1] J. C. Slonczewski, J. Magn. Magn. Mater. **159**, L1 (1996).
[2] L. Berger, Phys. Rev. B **54**, 9353 (1996).
[3] M. Tsoi, A. G. M. Jansen, J. Bass, W. C. Chiang, M. Seck, V. Tsoi, and P. Wyder, Phys. Rev. Lett. **80**, 4281 (1998); J. Z. Sun, Phys. Rev. B **62**, 570 (2000); J. A. Katine, F. J. Albert, R. A. Buhrman, E. B. Myers, and D. C. Ralph, Phys. Rev. Lett. **84**, 3149 (2000).
[4] S. I. Kiselev, J. C. Sankey, I. N. Krivorotov, N. C. Emley, R. J. Schoelkopf, R. A. Buhrman, and D. C. Ralph, Nature (London) **425**, 380 (2003).
[5] K.-J. Lee, A. Deac, O. Redon, J.-P. Nozières, and B. Dieny, Nature Mater. **3**, 877 (2004).
[6] B. Hillebrands and A. Thiaville, *Spin Dynamics in Confined Structures III* (Springer, New York, 2005).
[7] J. C. Slonczewski, U.S. Patent No. 5,695,864 (1997).
[8] I. Firastrau, D. Gusakova, D. Houssameddine, U. Ebels, M.-C. Cyrille, B. Delaet, B. Dieny, O. Redon, J.-Ch. Toussaint, and L. D. Buda-Prejbeanu, Phys. Rev. B **78**, 024437 (2008).
[9] V. S. Pribiag, I. N. Krivorotov, G. D. Fuchs, P. M. Braganca, O. Ozatay, J. C. Sankey, D. C. Ralph, and R. A. Buhrman, Nat. Phys. **3**, 498 (2007).
[10] Q. Mistral, M. van Kampen, G. Hrkac, J.-V. Kim, T. Devolder, P. Crozat, C. Chappert, L. Lagae, and T. Schrefl, Phys. Rev. Lett. **100**, 257201 (2008).
[11] S. Kasai, Y. Nakatani, K. Kobayashi, H. Kohno, and T. Ono, Phys. Rev. Lett. **97**, 107204 (2006).
[12] B. A. Ivanov and C. E. Zaspel, Phys. Rev. Lett. **99**, 247208 (2007).
[13] M. Bolte, G. Meier, B. Krüger, A. Drews, R. Eiselt, L. Bocklage, S. Bohlens, T. Tyliszczak, A. Vansteenkiste, B. V. Waeyenberge, K. W. Chou, A. Puzic, and H. Stoll, Phys. Rev. Lett. **100**, 176601 (2008).
[14] K. Yamada, S. Kasai, Y. Nakatani, K. Kobayashi, H. Kohno, A. Thiaville, and T. Ono, Nature Mater. **6**, 270 (2007).
[15] J.-G. Caputo, Y. Gaididei, F. G. Mertens, and D. D. Sheka, Phys. Rev. Lett. **98**, 056604 (2007).
[16] S.-K. Kim, Y.-S. Choi, K.-S. Lee, K. Y. Guslienko, and D.-E. Jeong, Appl. Phys. Lett. **91**, 082506 (2007).
[17] S.-K. Kim, K.-S. Lee, Y.-S. Yu, and Y.-S. Choi, Appl. Phys. Lett. **92**, 022509 (2008).
[18] K.-S. Lee, Y.-S. Yu, Y.-S. Choi, and S.-K. Kim, Appl. Phys. Lett. **92**, 192513 (2008).
[19] Y. Liu, H. He, and Z. Zhang, Appl. Phys. Lett. **91**, 242501 (2007).
[20] D. D. Sheka, Y. Gaididei, and F. G. Mertens, Appl. Phys. Lett. **91**, 082509 (2007).
[21] J. Miltat, G. Albuquerque, A. Thiaville, and C. Vouille, J. Appl. Phys. **89**, 6982 (2001).
[22] J. P. Strachan, V. Chembrolu, Y. Acremann, X. W. Yu, A. A. Tulapurkar, T. Tyliszczak, J. A. Katine, M. J. Carey, M. R. Scheinfein, H. C. Siegmann, and J. Stöhr, Phys. Rev. Lett. **100**, 247201 (2008).
[23] See http://llgmicro.home.mindspring.com.
[24] K.-S. Lee and S.-K. Kim, Phys. Rev. B **78**, 014405 (2008); K.-S. Lee and S.-K. Kim, Appl. Phys. Lett. **91**, 132511 (2007).
[25] K. Yu. Guslienko, K.-S. Lee, and S.-K. Kim, Phys. Rev. Lett. **100**, 027203 (2008).
[26] Exponentially decreasing or steady-state orbital motions can appear under specific conditions.
[27] From the present simulations, the critical current density is obtained as $j_{\mathrm{cri}}=6.4\times10^6$ A/cm^2 for STT only, $j_{\mathrm{cri}}=6.8\times10^6$ A/cm^2 for STT+OH(P), and 6.1×10^6 A/cm^2 for STT+OH(AP). These deviations for the case of additional OH effect are within ±5% of that for STT only.
[28] K. Y. Guslienko, B. A. Ivanov, V. Novasad, Y. Otani, H. Shima, and K. Fukamichi, J. Appl. Phys. **91**, 8037 (2002); K. Y. Guslienko, Appl. Phys. Lett. **89**, 022510 (2006).